Optica Applicata, Vol. XXXV, No. 2, 2005

X-ray carpal-bone image boundary feature analysis using region statistical feature based level set method for skeletal age assessment application

PAN LIN, CHONGXUN ZHENG, FENG ZHANG, YONG YANG

Institute of Biomedical Engineering, Xi'an Jiaotong University, Xi'an, 710049, P.R.China;
e-mail: linpan@mailst.xjtu.edu.cn

Skeletal age assessment is one of the important applications of hand radiography in the area of pediatric radiology. Feature analysis of the carpal-bones can reveal the important information for skeletal age assessment. The present work in this paper faces the problem of the detection of carpal -bone features from X-ray image. A novel and effective segmentation technique is presented in this work with carpal-bone image for skeletal age estimation. Carpal-bone segmentation is a critical operation of the automatic skeletal age assessment system. This method consists of two procedures. First, the original carpal-bone image is preprocessed via anisotropic diffusion filter. Then, the carpal-bone image is segmented by region based level set method. The basic idea of the region based level set method is to add a force that takes into account the information within the regions in order to add robustness and more efficiently separate homogeneous regions. Experiments are carried out on X-ray images of carpal-bone. The experimental results show that incorporating region statistical information into the level set method, an accurate and robust segmentation can be achieved.

Keywords: carpal-bone radiograph, skeletal age (estimation), anisotropic diffusion filter, level set method, region statistical information.

1. Introduction

Skeletal age assessment is widely applied to the area of pediatric radiology. There are two respected and widely-used methods for skeletal age assessment from hand wrist radiographs: the Greulich–Pyle (GP) method [1] and the Tanner–Whitehouse (TW2) method [2]. The doctors must observe the appearance and growth features of specific bones, and hence an empirically derived score, to each bone. The scores are summed up to give a net maturity rating, which, by reference to gender-dependent tables, may be converted into a "bone age" or estimated height at adulthood. However, the results of bone age assessment highly depend on the doctor's expertise and experience. Therefore, it is worthwhile to develop an automatic bone age assessment system to assist the doctor in performing a more objective and accurate assessment. Bone age

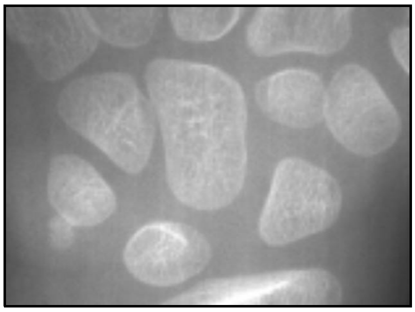

Fig. 1. X-ray image of a hand: **a** – original image, **b** – ROI of X-ray carpal-bone image.

assessment based on image processing can be divided into two phases. Phase one cosists in phalangeal and carpal-bone image feature extraction. Phase two is bone age assessment based on the features. Features of the carpal-bones (see Fig. 1) are important potential information for skeletal age assessment [3–6] in pediatric radiology. The recognition and separation of individual carpal-bone from the image of the carpal -bones is a very difficult task, we are faced with the presence of several overlapping regions of interest (ROI), the presence of ROI having completely different degree of calcification and overlapping with soft tissue, since different regions are of little gray level variations and the borders of individual carpal-bones are hardly visible.

A major requirement of the task is an efficient method to segment carpal-bones. Many techniques are actually available [3, 4]. With the techniques based on "classical" segmentation algorithms, such as region growing, edge detection, one usually cannot obtain accurate results. The complexity of the skeletal structure in the hand and the variability between different subjects makes it very difficult to realize an automatic segmentation of the carpal-bones. The level set approach was introduced by OSHER and SETHIAN [7] in 1988. This method has recently become one of the most studied techniques for medical image segmentation. Level sets are designed to handle problems in which the evolving interfaces can develop sharp corners and cusps, change topology and become very complex. This method has been found to be well adapted to our application, in particular because of this flexible initialization and its good convergence performances compared to other methods. A number of recent works [8–10] have sought to combine level set techniques with statistical approaches to segmentation. Much of this work has been motivated by the earlier work of CHAN and VESE [11] as well as ZHU and YUILLE [12]. Based on the Mumford-Shad segmentation, Chan and Vese introduced in a series of papers a new type of active contour models without gradient information. The curve evolution stopping term is actually a function that realizes the comparison of two image intensity terms inside the curve and outside the curve with the average intensity terms inside and outside the curve, respectively.

The main limitation of this model is that some objects cannot be detected only using the region intensity information. ZHU and YUILLE [12] have proposed a statistical framework model of region competition which combines the geometrical features of deformable models and the statistical nature of region growing. In this work, a new level set method framework is proposed, which is based on the image region statistical information. The main reason for this method was that the segmentation process takes advantage of the local and global shape information for pulling and pushing boundaries to capture the topology in the level set framework based on partial differential equations (PDE). Moreover, this method can be extended to more than two regions. In this paper, we present a novel and effective carpal-bone image segmentation method. This method is able to extract a variety of carpal-bone features. In order to improve the signal to noise ratio prior to segmentation the anisotropic non-linear diffusion filtering of images is used. The principle is to smooth out noise locally by diffusive flow while at the same time preventing the flow across object boundaries. Then we use the new region-based level set method to segment carpal-bone from digital X-ray image. The experimental results show that incorporating region intensity information into the level set framework, an accurate and robust segmentation can be achieved.

2. X-ray carpal-bone images preprocessing

X-ray can take carpal-bone images. Due to various factors, these images are in general poor in contrast, and image features in the cross sectional part are often obscured and degraded by artifacts. In order to obtain accurate and reliable feature information we applied image preprocessing to remove artifacts and degradations such as blurring and noise. For this reason we apply an anisotropic diffusion filter that smoothes noisy regions in the image while respecting edge boundaries. The principle is to smooth out noise locally by diffusive flow while at the same time preventing the flow across object boundaries.

Anisotropic diffusion filter was proposed by PERONA and MALIK [13]. The filtered image is modeled as the solution to the anisotropic diffusion equation

$$\frac{\partial I(p, t)}{\partial t} = \operatorname{div}\Big(G(p, t) \cdot \nabla I(p, t)\Big) \tag{1}$$

where $I(p, t)$ is the image intensity at position p and time t, ∇I is the spatial gradient, $\partial_t I$ is the temporal derivative and $G(p, t)$ is the conductance parameter. For $G = 1$ the the diffusion is linear, which has been shown to be equivalent to smoothing the image with a family of Gaussian filter kernels whose scale evolves to time t. Perona and Malik provided a solution to the problem, the resulting filter being based on the following equation:

$$I_{i,j}^{t+1} = I_{i,j}^{t} + \lambda\Big(c_U^t \nabla_U I_{i,j}^{t} + c_D^t \nabla_D I_{i,j}^{t} + c_L^t \nabla_L I_{i,j}^{t} + c_R^t \nabla_R I_{i,j}^{t}\Big) \tag{2}$$

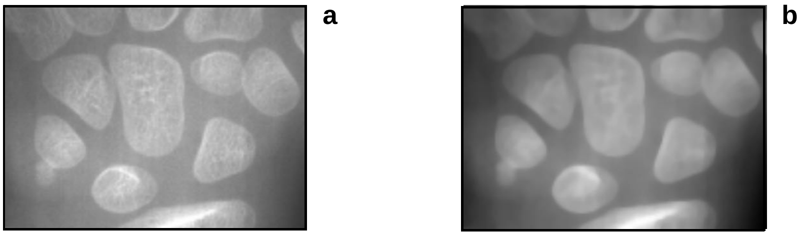

Fig. 2. Anisotropic smoothing of carpal-bones image: original carpal-bone image (**a**), anisotropic smoothing results (**b**).

where $I_{i,j}^t$ is the pixel value at position (i, j) at the time t, the coefficient $\lambda \in [0, 0.25]$, the terms ∇ are the finite differences calculated on a 4-connected neighborhood, and $c_U^t, c_D^t, c_L^t, c_R^t$ are the so-called conduction coefficients,

$$\nabla_U I_{i,j}^t = I_{i-1,j}^t - I_{i,j}^t, \quad \nabla_D I_{i,j}^t = I_{i+1,j}^t - I_{i,j}^t,$$

$$\nabla_L I_{i,j}^t = I_{i,j-1}^t - I_{i,j}^t, \quad \nabla_R I_{i,j}^t = I_{i,j+1}^t - I_{i,j}^t.$$

The diffusion coefficient $G(p, t)$ then adaptively controls the diffusion strength, smoothing the image within a moderately continuous region while not smoothing across sharp discontinuities. The diffusion process achieves piecewise smoothing while preserving the relevant image edges. The conductivity model suggested in [14] is used in our experiments, thus:

$$G(p, t) = \exp\left(-\frac{\|\nabla I(p)\|}{k}\right). \tag{3}$$

The parameter k determines the local behavior of the filter: smoothing if $\|\nabla I\| \le k$ and edge sharpening if $\|\nabla I\| > k$.

Edge-preserving smoothing prior to subsequent analysis yielded more robust results. Figures 2**a** and 2**b** show the original carpal-bone image and the anisotropic smoothing results, respectively.

3. Level set method model

The level set method was devised by OSHER and SETHIAN [7]. The main idea in the level set method is to describe a closed curve Γ in the image plane as the zero level set of a higher dimensional function $\phi(x, t)$ in $\Re^3$. The value of function ϕ at some point x is defined by

$$\phi(x, t = 0) = \pm d \tag{4}$$

where d is the distance from x to $\Gamma(t = 0)$, and the sign is chosen whether the point x lies outside or inside the initial hypersurface $\Gamma(t = 0)$. In this manner, Γ is represented by the zero level set $\Gamma(t) = \{x \in R^2 | \phi(x, t) = 0\}$ of the level set function, and the initial function $\phi(x, t = 0)$ with the property that $\Gamma(0) = \{x \in R^2 | \phi(x, t = 0) = 0\}$. The evolution of $\phi(x, t)$ can be modelled as :

$$\frac{\partial \phi}{\partial t} + F\|\nabla \phi\| = 0 \quad \text{with} \quad \phi(x, t = 0). \tag{5}$$

The speed function F plays the major role in the evolution process. The speed function F depends on factors like the image gradient. A common choice for F is:

$$F = P(I)(1 - \varepsilon k) \tag{6}$$

where $0 < \varepsilon < 1$ is a constant, I is the image intensity and k is the curvature obtained from divergence of the gradient of the normal vector to the front; curvature k can be defined as:

$$k = \operatorname{div}\left(\frac{\nabla \phi}{|\nabla \phi|}\right) = \frac{\phi_{xx}\phi_y^2 - 2\phi_x\phi_y\phi_{xy} + \phi_{yy}\phi_x^2}{\left(\phi_x^2 + \phi_y^2\right)^{3/2}}. \tag{7}$$

The term $P(I)$ is an image-dependent halting criterion calculated as:

$$P(I) = \exp\left(-\left|\nabla G_\sigma \cdot I\right|\right) \tag{8}$$

where $\nabla G_\sigma \cdot I$ denotes the image convolved with a Gaussian smoothing filter whose characteristic width is σ. This halting criterion allows the modelling to stop at high image gradient by reducing the speed function to zero, thus aligning it to the object boundary.

Given the initial value, the problem can be solved by means of difference operators in a fixed grid via

$$\phi_{ij}^{n+1} = \phi_{ij}^{n} - \Delta t\, h\left[\max(F_{ij}, 0)\nabla^{+} + \min(F_{ij}, 0)\nabla^{-}\right] \tag{9}$$

where n is the iterative time, h is the grid step, Δt is the time step, F_{ij} is the speed value of pixel (i, j), ϕ_{ij}^{n} is the level value of pixel (i, j) at time n and where

$$\nabla^{+} = \left[\max(D_{ij}^{-x}\phi, 0)^2 + \min(D_{ij}^{+x}\phi, 0)^2 + \max(D_{ij}^{-y}\phi, 0)^2 + \min(D_{ij}^{+y}\phi, 0)^2\right]^{\frac{1}{2}} \tag{10}$$

$$\nabla^- = \left[\max(D_{ij}^{+x}\phi, 0)^2 + \min(D_{ij}^{-x}\phi, 0)^2 + \max(D_{ij}^{+y}\phi, 0)^2 + \min(D_{ij}^{-y}\phi, 0)^2\right]^{\frac{1}{2}} \tag{11}$$

$$D_{ij}^{-x}\phi = \frac{\phi_{ij}^n - \phi_{(i-1)j}^n}{\Delta x}, \quad D_{ij}^{+x}\phi = \frac{\phi_{(i+1)j}^n - \phi_{ij}^n}{\Delta x}, \tag{12}$$

$$D_{ij}^{-y}\phi = \frac{\phi_{ij}^n - \phi_{i(j-1)}^n}{\Delta y}, \quad D_{ij}^{+y}\phi = \frac{\phi_{i(j+1)}^n - \phi_{ij}^n}{\Delta y}. \tag{13}$$

This implementation allows the function ϕ to automatically follow topological changes and corners during evolution.

4. Region statistical feature based level set method

However, gradient information has no meaning for very noisy and low contrasted images. Besides, high gradients do not necessarily indicate a relevant boundary between the structure to be segmented and its background. The key idea was to utilize the region intensity information inside and outside the structure to be segmented. The pixel in the neighborhood of the segmenting structure was responsible for creating a pull/push force on the propagating front.

4.1. Image region prior models descriptors

We consider a deformable model, which consists of a partition of the image domain into three subsets: object and background and their common boundary (shown in Fig. 3)

$$\Omega = \Omega_{\text{in}} \cup \Omega_{\text{out}} \cup C. \tag{14}$$

In many cases, not only the observed measurements along the contour but also the gray-levels inside and outside the object contain information, for instance when the average gray-level inside the object is very different from the average gray-level outside the object.

The goal is to segment the domain Ω of a given image into two "homogeneous" regions separated by the contour C. The region inside the contour Ω_{in} represents the object region. The region outside the contour Ω_{out} corresponds to the background region. We partition the image pixels $\{(i, j) \in \Omega\}$ into two groups separated by the contour C. Our objective then is to process the observed image gray values $I(x, y)$ in order to estimate the partitions R_O and R_B

$$I(x, y) = \begin{cases} R(I_O) & \text{if} \quad x \in \text{object} \\ R(I_B) & \text{if} \quad x \notin \text{object} \end{cases} \tag{15}$$

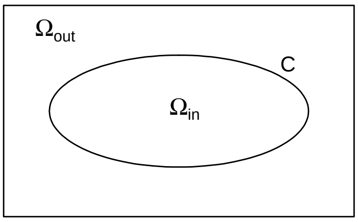

Fig. 3. Illustration of the contour (C), the region inside the contour (Ω_{in}) and the region outside the contour (Ω_{out}).

where $R(I_O)$ represents the object region structure and $R(I_B)$ represents the background region structure; I_O and I_B represent the object and background pixel values, respectively.

As discussed in [15], the maximum likelihood estimation of the target shape can be obtained by maximizing the likelihood

$$p(R(I)|I) = p(\{R(I_O), R(I_B)\}|I) \tag{16}$$

where $R(I_O)$ and $R(I_B)$ are the set of pixels inside and outside the contour, respectively, and are specified by $I(x, y)$. Let us consider the case where the image $I(x, y)$ could be the Gaussian distribution. Assuming that this probability density function is homogeneous, we can write:

$$p[I(x, y)] = \frac{1}{\sqrt{2\pi}\,\sigma} \exp\left[-\frac{(I(x, y) - \mu)^2}{2\sigma^2}\right] \tag{17}$$

where μ and σ are the mean and the variance of the image region. In this work, it is assumed that the intensity distribution over the image is bimodal, *i.e.*, the object to be segmented and its background. So, we can get the probability function of the object and background as follows:

$$p_O(x, y) = \frac{1}{\sqrt{2\pi}\,\sigma_O} \exp\left[-\frac{(I(x, y) - \mu_O)^2}{2\sigma_O^2}\right], \tag{18}$$

$$p_B(x, y) = \frac{1}{\sqrt{2\pi}\,\sigma_B} \exp\left[-\frac{(I(x, y) - \mu_B)^2}{2\sigma_B^2}\right] \tag{19}$$

where $p_O(x, y)$ and $p_B(x, y)$ denote the likehood of intensity inside and outside the object (μ_O, μ_B, σ_O^2 and σ_B^2 are, respectively, the mean and the variance of the image intensity).

Here we make the assumption of image $I(x, y)$, in which object and background are independently drawn from a Gaussian mixture distribution, respectively. According to the Bayes rule the probabilities of this region depend only on their observation data set given as:

$$p(R(I)|I) = p(I|R(I_O))p(I|I_B) = \prod_{(x,y) \in R(I_O)} p_O(x,y) \prod_{(x,y) \in R(I_B)} p_B(x,y) \tag{20}$$

where $p(I|R(I_O))$ and $p(I|R(I_B))$ are the posteriori probabilities for the object and background region. The maximization of the a posteriori segmentation probability (19) is equivalent to the minimization of the following region energy function:

$$E_R(x,y) = \sum_{(x,y) \in R_O} \left[\frac{-(I(x,y) - \mu_O)^2}{2\sigma_O^2} - \log\sqrt{2\pi}\,\sigma_O\right] + \sum_{(x,y) \in R_B} \left[\frac{-(I(x,y) - \mu_B)^2}{2\sigma_B^2} - \log\sqrt{2\pi}\,\sigma_B\right]. \tag{21}$$

The corresponding parameters (μ_r, σ_r) of the image pixel from inside and outside contour C are estimated using maximum likelihood (ML) algorithm [15].

$$\hat{\mu}_r = \frac{1}{N}\sum_{x \in r} I(x,y) \tag{22}$$

and

$$\hat{\sigma}_r^2 = \frac{1}{N}\sum_{x \in r} I(x,y)^2 - \hat{\mu}_r^2. \tag{23}$$

4.2. Energy functional

Here, we combine the region statistical information estimate with curvature-based regularization penalizing the length of curve. A minimal length penalty is adapted to regularize such an evolution process [16] since small sacrifices regarding the data consistency term minimization will allow the smoothing of the main contours and shrinking of the small contours until they vanish. In the 2-D case, this penalty is expressed through the following criterion:

$$L = \lambda \oint_{\mathbf{C}} \mathrm{d}s \tag{24}$$

where $\oint_{\mathbf{C}} \mathrm{d}s$ is the length of the curve and λ is a scalar parameter. In order to regularize the contour, we add a length term to the region energy term (21). Thus, the segmentation problem is then the solution to the variation problem of finding the partition image region that minimizes the following energy function:

$$E_{\Omega} = E_R(x, y) + L = E_R(x, y) + \lambda \oint_{\mathbf{C}} \mathrm{d}s \tag{25}$$

where E_{Ω} is the total energy, $E_R(x, y)$ is the region energy, $\lambda \oint_{\mathbf{C}} \mathrm{d}s$ is the contour smoothing term.

4.3. Level set implementation

In order to minimize the above energy, now a level set function [7] is introduced. Let $\phi: \Omega \to R$ be the level set function with $\phi(x) > 0$ if $x \in \Omega_{\text{in}}$ and $\phi(x) < 0$ if $x \in \Omega_{\text{out}}$. The zero level line of ϕ is the boundary between the two regions. Then, from the previous description, we can deduce the evolution of the curve contour that will evolve towards a minimum of the energy function E_{Ω} defined in (25). According to (5), we find the following evolution equation:

$$\frac{\partial \phi}{\partial t} + F \|\nabla \phi\| = 0. \tag{26}$$

Thus, this leads to the following curve evolution PDE:

$$\frac{\partial \phi}{\partial t} + \left\{ \frac{1}{2} \left[\log(\sigma_O^2) - \log(\sigma_B^2) + \frac{(I(x, y) - \mu_O)^2}{\sigma_O^2} + \frac{(I(x, y) - \mu_B)^2}{\sigma_B^2} \right] - \lambda k \right\} |\nabla \phi| = 0 \tag{27}$$

where λ is a parameter that modifies the influence of regularization, where k is the curve at the boundary of the region, and it is computed as the divergence of the unit normal function to the curve:

$$k = \operatorname{div}\left(\frac{\nabla \phi}{|\nabla \phi|} \right). \tag{28}$$

In the case of time independent region statistical descriptors, the speed function F that minimizes the energy functional is consequently given by:

$$F = \frac{1}{2} \left[\log(\sigma_O^2) - \log(\sigma_B^2) + \frac{(I(x, y) - \mu_O)^2}{\sigma_O^2} + \frac{(I(x, y) - \mu_B)^2}{\sigma_B^2} \right] - \lambda k. \tag{29}$$

The first term is a region likelihood ratio test, which compares the hypotheses that the observed image intensity at a given point on the curve contour belongs to the object region or background region based on the current estimates. The second term is the curve length penalty.

5. Experimental results

In this section, we examine the performance of image segmentation method described in the previous sections. Several experiments have been done to examine the performance of level set method for carpal-bones image segmentation. Carpal-bones image segmentation is important for skeletal age assessment. The first stage refers to modelling stage where the observed histogram is approximated using Gaussian mixture model. This analysis denotes the region statistics. Then the segmentation process is performed by employing the region-based level set model. The region boundary is determined using a probability module by searching for local discontinuities on the statistical space that is associated with the image feature. The model deals automatically with changes of topology. The curve evolution equation allows any point on a closed curve segment to evolve according to the region force determined by the intensity of the original image. The corresponding numerical algorithm used is summarized as follows:

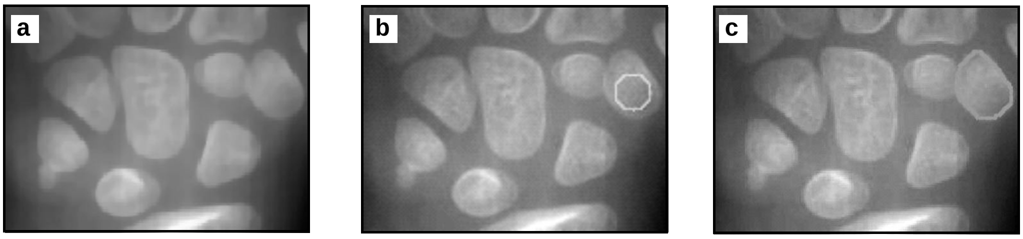

Fig. 4. Segmentation of two overlapping carpal-bone features (**a**) original image (**b**) initial contour (**c**) segmented by the level set method.

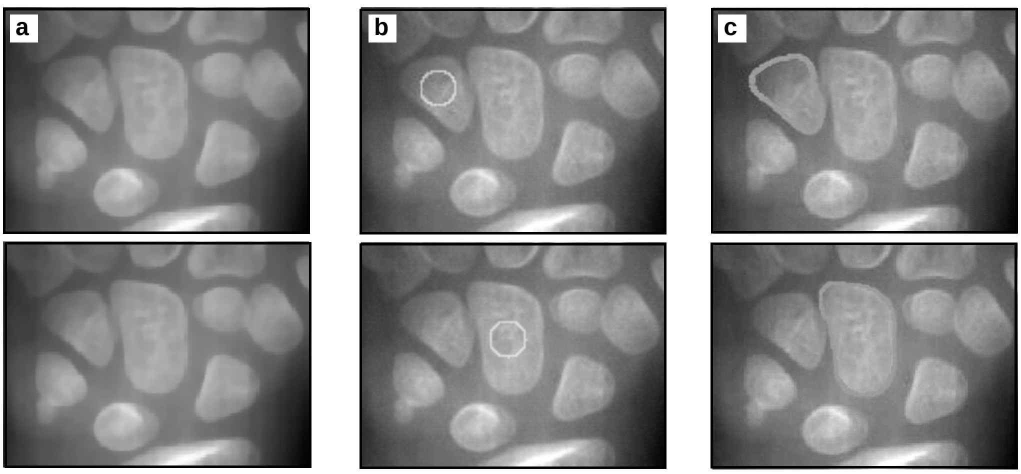

Fig. 5. Carpal-bone contour feature extraction (**a**) original image (**b**) initial contour (**c**) segmented by the level set method.

1) according to the region to be segmented, make initial curve contour;

2) according the each separated region, using ML estimate its mean and variance;

3) compute the speed function F using the estimated object region and background statistical information;

4) make the level set function evolve according to the new speed function F to obtain a new contour;

5) repeat steps 2) to 5) until the curve contour is converged.

However, different regions are of little gray-level variations and the borders of individual carpal-bones are hardly visible. In this experiment, our aim is to extract the boundary of shapes characterized by a gray-level intensity different from the surroundings. Figure 4 illustrates an important aspect about this segmentation technique. Two carpal-bones that overlap each other are shown. Most other segmentation methods are based on the assumption that a pixel can belong to one and only one object. Using the level set method no such limitations apply and two overlapping objects can be both perfectly segmented. Figure 4**a** is the original carpal -bone image, Fig. 4**b** shows the initial curve contour, Fig. 4**c** shows the final segmentation results.

The extraction of other carpal-bone shape features is shown in Fig. 5. Figure 5**a** shows the original image, Fig. 5**b** shows the initial contour, Fig. 5**c** shows the segmentation result.

Experimental results show that incorporating region statistical information into the level set framework, an accurate and robust X-ray carpal-bone segmentation can be achieved.

6. Conclusions

In this paper, a region based level set approach to carpal-bone segmentation from digital X-ray images is proposed. The novel method developed can correctly extract the carpal-bone feature from X-ray image. The anisotropic diffusion filter can effectively reduce noise from X-ray image without deteriorating the actual bone boundaries. The complexity of the skeletal structure in the hand and the variability between different subjects makes it very difficult to realize an automatic segmentation of the bones. The level set method provides a powerful framework for carpal-bone image segmentation. The experiments are carried out on images of carpal-bone and the results are very promising. This method could be extended and applied to other bone structures as well as to other images.

References

[1] Greulich W.W., Pyle S.I., *Radiographic Atlas of Skeletal Development of the Hand and Wrist*, 2nd Ed., Stanford University Press, Palo Alto, CA 1959.

[2] Tanner J.M., Whitehouse R.H., Marshall W.A., Healy M.J.R., *Assessment of Skeletal Maturity and Prediction of Adult Height (TW2 Method)*, 2nd Ed., Academic Press, London 1983.

[3] PIETKA E., KAABI L., KUO M.L., HUANG H.K., *Feature extraction in carpal-bone analysis*, IEEE Transactions on Medical Imaging. **12**(1), 1993, pp. 44–9.

[4] KO C.C., MAO C.W., LIN C.J., SUN Y.N., *Image analysis for skeletal evaluation of carpal bones*, Proceedings of the SPIE **2501**, pt. 2, 1995, pp. 951–61.

[5] MICHAEL D.J., NELSON A.C., *HANDX: A model-based system for automatic segmentation of bones from digital hand radiographs*, IEEE Transactions on Medical Imaging **8**(1), 1989, pp. 64–9.

[6] EFFORD N.D., *Knowledge-based segmentation and feature analysis of hand wrist radiographs*, [In] *School of Computer Studies, Research Report Series*, University of Leeds, Report 94.31, 1994.

[7] OSHER S.J., SETHIAN J.A., *Fronts propagating with curvature dependent speed: Algorithms based on Hamilton–Jacobi formulations*, Journal of Computational Physics **79**(1), 1988, pp. 12–49.

[8] CHAKRABORTY A., STAIB L., DUNCAN J., *Deformable boundary finding in medical images by integrating gradient and region information*, IEEE Transactions on Medical Imaging **15**(6), 1996, pp. 859–70.

[9] CHAN T.F., VESE L.A., *Active contours without edges*, IEEE Transactions on Image Processing **10**(2), 2001, pp. 266–77.

[10] PARAGIOS N., DERICHE R., *Geodesic active regions for supervised texture segmentation*, Proceedings of ICCV, Sept. 1999, Corfu, Greece.

[11] CHAN T., VESE L., *An active contour model without edges*, [In] *Lecture Notes in Computer Science, Proceedings of the Second International Conference on Scale-Space Theories in Computer Vision*, [Eds.] M. Nielsen, P. Johansen, O.F. Olsen, J. Weickert, Vol. 1682, 1999, pp. 141–51.

[12] ZHU S.-C., YUILLE A., *Region competition: Unifying snakes, region growing, and Bayes/MDL for multiband image segmentation*, IEEE Transactions on Pattern Analysis and Machine Intelligence **18**(9), 1996, pp. 884–900.

[13] PERONA P., MALIK J., *Scale-space and edge detection using anisotropic diffusion*, IEEE Transactions on Pattern Analysis and Machine Intelligence **12**(7), 1990, pp. 629–39.

[14] GERMAIN O., REFREGIER P., *Optimal snake-based segmentation of a random luminance target on a spatially disjoint background*, Optical Letters **21**(22), 1996, pp. 1845–7.

[15] DEMPSTER A.P., LAIRD N.M., RUBIN D.B., *Maximum-likelihood from incomplete data via the EM algorithm*, Journal of the Royal Statistical Society B **39**, 1977, pp.1–38.

[16] GUILLERMO SAPIRO, *Geometric Partial Differential Equations and Image Analysis*, Cambridge University Press 2001.

Received January 5, 2005
in revised form March 13, 2005